



Melatonin fine-tunes intracellular calcium signals and eliminates myocardial damage through the IP3R/MCU pathways in cardiorenal syndrome type 3

Jin Wang^a, Sam Toan^{b,c}, Ruibing Li^a, Hao Zhou^{a,*}

^a Chinese PLA General Hospital, Medical School of Chinese PLA, Beijing 100853, China

^b Center for Cardiovascular Research and Alternative Medicine, University of Wyoming College of Health Sciences, Laramie, WY 82071, USA

^c Department of Chemical Engineering, University of Minnesota-Duluth, Duluth, MN 55812, USA

ARTICLE INFO

Keywords:

CRS-3
Melatonin
IP3R
MCU
Calcium overload
Mitochondria

ABSTRACT

Cardiorenal syndrome type-3 (CRS-3) is characterized by acute cardiac injury induced by acute kidney injury. Here, we investigated the causes of CRS-3 by analyzing cardiac function after renal ischemia–reperfusion injury (IRI) using echocardiography and evaluation of pro-inflammatory markers, calcium balance, mitochondrial function, and cardiomyocyte death. Our results show that renal IRI reduces cardiac diastolic function associated with cardiomyocyte death and inflammatory responses. Renal IRI also disrupts cardiomyocyte energy metabolism, induces calcium overload, and impairs mitochondrial function, as evidenced by reduced mitochondrial membrane potential and increased mitochondrial fission. Further, renal IRI induces phosphorylation of inositol 1,4,5-trisphosphate receptor (IP3R) and expression of mitochondrial calcium uniporter (MCU), resulting in cytoplasmic calcium overload and mitochondrial calcium accumulation. Pretreatment with melatonin attenuates renal IRI-mediated cardiac damage by maintaining myocardial diastolic function and reducing cardiomyocyte death. Melatonin also inhibits IP3R phosphorylation and MCU expression, thereby alleviating cytoplasmic and mitochondrial calcium overload. Blockade of IP3R has similar cardioprotective effects, whereas MCU activation abrogates the melatonin-mediated cardioprotection. These results show that the negative effects of renal IRI on myocardial viability and cardiac function are caused by induced IP3R phosphorylation, MCU upregulation, and calcium overload. Melatonin protects cardiac function against CRS-3 by suppressing IP3R-MCU signaling.

1. Introduction

Cardiorenal crosstalk dysfunction can lead to diabetes, hypertension, atherosclerosis, amyloidosis, cirrhosis, and septic shock [1]. One in six patients with stage 4 chronic kidney disease suffers from heart failure [2,3]. On the other hand, half of patients with acute heart failure have some degree of renal insufficiency [4,5]. Renal blood perfusion is controlled by the amount of blood the heart pumps through the circulatory system, whereas most myocardial metabolic wastes are rapidly excreted by the kidneys through glomerular filtration or active tubular secretion [6]. The concurrence of a cardiovascular disorder and kidney dysfunction is a result of a complex pathophysiological mechanism that raises significant problems for clinicians. The cardiorenal syndrome type-3 (CRS-3) is a subtype of CRS characterized by an acute cardiac injury caused by acute kidney injury [7,8]. However, our understanding of the pathological mechanisms underlying CRS-3 is limited, and no targeted therapeutic approaches are available to improve the myocardial function.

The biophysical and biochemical mechanisms of CRS-3 include inflammation, oxidative stress, metabolic alteration of cardiomyocytes, neuroendocrine activation, electrophysiological abnormalities in cardiomyocytes, and mitochondrial dysfunction [9,10]. Interestingly, these pathophysiological processes are regulated by melatonin, a hormone released by the pineal gland that controls the natural sleep-wake cycle [11,12]. The cardioprotective effects of melatonin have been shown in various models of acute cardiac dysfunction, such as cardiac ischemia reperfusion injury (IRI), septic cardiomyopathy [13], viral myocarditis [14], and drug-induced cardiotoxicity [15]. However, there is no evidence to support the use of melatonin as a targeted therapeutic tool for CRS-3-caused acute cardiac dysfunction.

The biophysical and biochemical properties of cardiomyocytes are regulated by calcium oscillations and mitochondria-produced ATP via oxidative phosphorylation. Abnormal calcium transport is associated with baseline Ca^{2+} overload and a decreased peak concentration of intracellular Ca^{2+} ($[\text{Ca}^{2+}]_i$), which impairs the diastolic and systolic functioning of the left ventricle [16,17]. In addition, aberrant calcium

* Corresponding author at: Chinese PLA General Hospital, Medical School of Chinese PLA, Beijing 100853, China.

E-mail address: zhouhao@plagh.org (H. Zhou).

<https://doi.org/10.1016/j.bcp.2020.113832>

Received 8 November 2019; Accepted 27 January 2020

0006-2952/© 2020 Elsevier Inc. All rights reserved.

transport drives mitochondrial calcium ($[Ca^{2+}]_m$) overload, which induces cardiomyocyte death because the excessive $[Ca^{2+}]_m$ accumulation decreases oxidative phosphorylation-mediated ATP production by interacting with phosphate groups [18,19]. In cardiomyocytes, the intracellular Ca^{2+} signaling is primarily regulated by inositol 1,4,5-trisphosphate receptor (IP3R) and mitochondrial calcium uniporter (MCU) [20,21]. IP3R is localized on the surface of endoplasmic reticulum (ER), whereas MCU is expressed on the outer mitochondrial membrane. Our previous studies indicated that IP3R upregulation, driven by cardiac ischemia–reperfusion injury (IRI), is responsible for cardiomyocyte viability reduction and myocardial dysfunction [22]. Further, IP3R-mediated $[Ca^{2+}]_i$ disorder is associated with a $[Ca^{2+}]_m$ overload and increased cardiomyocyte death; however, the mechanism is unknown [23]. Interestingly, therapeutic delivery of melatonin provides an obvious heart-protective effect through the reorganization of $[Ca^{2+}]_i/[Ca^{2+}]_m$ homeostasis [24,25]. This is consistent with previous studies indicating that melatonin could reverse the amplitude and decay time of calcium transients in hypoxia/ischemia-treated cardiomyocytes [26]. In addition, the regulatory action of melatonin on calcium homeostasis has been demonstrated in cancer [27], erythrocytes [28], endothelial cells [29], neurodegenerative diseases [30], and the pancreas [31]. In this study, we investigated the pathological roles of $[Ca^{2+}]_i/[Ca^{2+}]_m$ disturbance and IP3R/MCU pathway in CRS-3-related cardiac dysfunction, and explored the potential of melatonin as a novel cardioprotective agent in acute renocardiac attack.

2. Materials and methods

2.1. Chemicals and reagents

Isoflurane (Cat. No. 792632, St Louis, MO, USA), DMSO (Cat. No. D2650, St Louis, MO, USA), melatonin (Cat. No. M5250, St Louis, MO, USA), and MTT (Cat. No. M2003, St Louis, MO, USA) were purchased from Sigma-Aldrich. BAPTA-AM (Cat. No. S7534, Selleck Chemicals, Houston, TX, USA) and spermine (Cat. No. S5522, Selleck Chemicals, Houston, TX, USA) were purchased from Selleck Chemicals. Dulbecco's modified Eagle medium (DMEM), fetal bovine serum (FBS), Pierce LDH Cytotoxicity Assay Kit (Cat. No. #88953), Fura-2 (Cat. No. F1201), and Rhod-2 (Cat. No. R1244) were purchased from Thermo Fisher Scientific. Penicillin-streptomycin was purchased from GENOM (Hangzhou, China). ATP Bioluminescent Assay Kit (Cat. No. S0027, China, Beyotime Biotechnology), Penicillin-streptomycin (Cat. No. C0222, China, Beyotime Biotechnology), and Mitochondrial Membrane Potential JC-1 Kit (Cat. No. C2006, China, Beyotime Biotechnology) were purchased from Beyotime Biotechnology. Xestospongins C (Cat. No. ab120914) was purchased from Abcam.

2.2. Mouse studies

Eight-week-old male C57BL/6 mice were purchased from the Laboratory Animal Center, Chinese PLA General Hospital. The mice were housed in a temperature-controlled room under 12/12 h light/dark cycle and had a free access to natural-ingredient food and water. Acute kidney ischemia–reperfusion injury (IRI) was induced by a 30-min bilateral renal artery ischemia, followed by 24 h or 72 h reperfusion. To avoid potential gender-related variations, all experiments were performed in male mice. Mice (eight-week-old) were anesthetized with 1%–3% isoflurane through inhalation (Baxter, Deerfield, IL). Thirty minutes after renal IRI surgery, the mice were intraperitoneally injected with melatonin (Sigma-Aldrich, St. Louis, MO, USA, 20 mg/kg) ($n = 6$ /group). To inhibit IP3R activation, a single intraperitoneal (i.p.) injection of thapsigargin at 1 mg/kg was used 30 min after renal ischemia surgery. In addition, to activate MCU in melatonin-treated mice, spermidine i.p. treatment at 5 mg/kg was used 30 min after renal ischemia surgery [32]. The mice were euthanized 24 and 72 h after reperfusion. Blood, kidney, and heart specimens were taken for analysis. To analyze

the histological alterations, paraffin-embedded heart tissues were cut into sections 5 μ m thick and stained with H&E.

2.3. Echocardiographic measurements in vivo

Mice were anesthetized using isoflurane inhalation, and echocardiographic functions were examined using the Vevo 2100 system (VisualSonics, Toronto, Canada), as previously described [33]. M-mode images were obtained from a parasternal short-axis view at the mid-ventricular level with a clear view of the papillary muscle. Interventricular septum depth at end diastole (IVSd), interventricular septum depth at end systole (IVSs), left ventricular internal diameter at end diastole (LVIDd), left ventricular internal dimension at end systole (LVIDs), left ventricular posterior wall depth at end diastole (LVPWd), left ventricular posterior wall depth at end systole (LVPWs), left ventricular ejection fraction (LVEF), left ventricular fractional shortening (LVFS), left ventricular mass (LVM), left ventricular end diastolic volume (LVEDV), left ventricular end systolic volume (LVESV), and E/A value were measured [34]. All measurements were performed in accordance with the American Society for Echocardiology's leading-edge techniques and standards, and the values of three consecutive cardiac cycles were averaged [35].

2.4. Western blotting

Heart tissues or cardiomyocytes were lysed in lysis buffer containing a protease inhibitor cocktail (Beyotime Institute of Biotechnology). Equal amounts of protein for cell lysates (20 μ g) and for heart tissues were loaded onto SDS-PAGE gel, resolved, and transferred to nitrocellulose membrane. The membrane was incubated overnight with primary antibodies diluted in TBS-T containing 5% blotting-grade blocker (Bio-Rad) or 5% BSA for phosphorylated proteins [36]. The blots were developed and detected using chemiluminescence (Millipore). The antibodies used in our study were as follows: p-IP3R (#8548, 1:1000, Cell Signaling Technology), t-IP3R (#8568, 1:1000, Cell Signaling Technology), GAPDH (#5174, 1:1000, Cell Signaling Technology), t-Drp1 (#5391, 1:1000, Cell Signaling Technology), p-Drp1 (#PA5-64821, 1:1000, Thermo Scientific Fisher), TNF α (#11948, 1:1000, Cell Signaling Technology), IL-6 (#12912, 1:1000, Cell Signaling Technology), and TGF β (#5544, 1:1000, Cell Signaling Technology).

2.5. RNA isolation and qRT-PCR analysis

Total heart tissue or cardiomyocyte RNA was isolated using TRIzol reagent (Invitrogen) and RNeasy Mini Kit (Qiagen) following the manufacturer's protocol [37]. Subsequently, 1 μ g of the total RNA was reverse transcribed to cDNA using the QuantiTect Reverse Transcription Kit (Qiagen), and qPCR was performed in duplicates using iTaq SYBR Green (Bio-Rad) on an Applied Biosystems 7500 Fast qRT-PCR system. Standard curves with pooled cDNA were used to calculate amplification efficiencies [38], and relative gene expression was normalized to GAPDH. The primer sequences were as follows: IP3R (Forward, GAGATGAGCCTGGCTGAGGTTCAA; Reverse, TGTTGCCTCCTTCAGAAGTGGCA), MCU (Forward: GCAACTTCAGCATATGACC; Reverse, GGAATTGGGATGCCATAGC), NCX (Forward, TTCTCATACTCC TCGTCATCG; Reverse, TTGAGGACACCTGTGGAGTG), Mif (Forward, AAGTGGCTCTCACCTAGCA; Reverse, TGCCCCACTCACCAAATGT) Fis1 (Forward, CAAGGAAGTGGAGCGGCTCATT; Reverse, GGACACA GCAAGTCCGATGAGT), MMP9 (Forward, AAGGACGGCCTTCTGGCAC ACGCCTTT; Reverse, GTGGTATAGTGGGACACATAGTGG), IL1 β (Forward, AGTTGACGGACCCCAAAAGAT; Reverse, GTTGTGTGCTGCTGCGAGA), MIP1 α (Forward, CCACTCACCTGCTGCTACTC; Reverse, AAGGCATCACAGTCCGAGTC).

2.6. Cardiomyocyte culture and shortening/relengthening assay *in vitro*

Primary cardiomyocytes were isolated from mice after renal IRI surgery or melatonin treatment, using trypsin and collagenase, as previously described [39]. In brief, mice heart tissues were treated with 0.1% (w/v) collagenase for 20 min at 37°C, and then incubated with 0.25% (w/v) trypsin overnight at 4°C. The cardiomyocytes were subsequently plated at a density of 5×10^5 cells/ml in DMEM supplemented with 15% (v/v) fetal bovine serum (FBS) at 37°C and 5% (v/v) CO₂. The cardiomyocytes were maintained in DMEM supplemented with 20% FBS and antibiotics (100 U/ml penicillin and 100 mg/ml streptomycin) in a humidified incubator. BAPTA-AM at 5 μM was used *in vitro* to inhibit the calcium overload. Single cardiomyocyte contractile parameters were evaluated using a SoftEdge MyoCam system (IonOptix, Milton, MA) [40]. After the evaluation of resting cellular length, the cardiomyocytes' peak shortening (PS), time-to-PS (TPS), time-to-90% relengthening (TR90), and maximal velocity of shortening/relengthening (\pm dL/dt) were determined (n = 70–90 cells/group).

2.7. Cardiomyocyte viability measurement *in vitro*

In vitro, cardiomyocyte viability was determined via MTT (3-(4, 5-dimethylthiazol-2-yl)-2,5-diphenyl-tetrazolium bromide) assay and lactate dehydrogenase (LDH) release assay [41]. In MTT assay, a total of 50,000 cardiomyocytes were transferred to a 96-well flat-bottom plate. After overnight incubation, the cells were incubated 4 h at 37 °C in a culture medium containing 10 μl MTT, and absorbance at 570 nm was measured in triplicates. To measure the levels of LDH in the cardiomyocyte culture medium, Pierce LDH Cytotoxicity Assay Kit (Thermo Fischer Scientific, #88953) was used in accordance with the manufacturer's protocol [42]. To determine the background LDH release, the complete culture medium without cardiomyocytes was utilized. The absorbance was measured at 490 nm.

2.8. Immunofluorescence assay

Cardiomyocytes were seeded on glass coverslips and cultured for 24 h at 37°C and 5% (v/v) CO₂. Then, cardiomyocytes on glass coverslips were fixed with 4% paraformaldehyde for 10 min, permeabilized with 0.3% Triton X-100 for 5 min, and blocked with 10% goat serum albumin (Invitrogen) for 1 h at room temperature. Subsequently, cardiomyocytes were incubated overnight at 4 °C with anti-Tom 20 primary antibody (Abcam, #ab186735) diluted 1:1,000 in 1% BSA. After washing in PBS for three times, cardiomyocytes were incubated with fluorochrome-coupled secondary antibody (Life Technologies #A11030, #A11034) for 1 hr at room temperature. Nuclei were stained with DAPI. The target protein expression was visualized under a Zeiss LSM 700 confocal laser scanning microscope (Carl Zeiss, Germany) with a 60x oil immersion objective. Images were captured using ZEN software (Carl Zeiss, Germany) [43].

To measure the levels of mitochondrial calcium ($[Ca^{2+}]_m$) and cytoplasmic calcium ($[Ca^{2+}]_c$), live cardiomyocytes, cultured in a 6-well plate, were incubated with Fluo-2 (Thermo Fisher Scientific) and Rhod-2 (Thermo Fisher Scientific) for 30 min at 37 °C in accordance with the manufacturer's instructions [44]. The fluorescence intensity of Fluo-2 and Rhod-2 was measured using excitation wavelengths of 340 and 550 nm, and emission wavelengths of 500 and 570 nm, respectively [45]. Data (F/F₀) were obtained by dividing fluorescence intensity (F) by (F₀) at resting level (t = 0), which was normalized by control groups. The mean fluorescent intensity was analyzed using ImageJ Version 10.2.

2.9. TUNEL staining

Cardiomyocytes were seeded on glass coverslips and cultured for 24 h at 37°C and 5% (v/v) CO₂. Then, cardiomyocytes on glass

coverslips were fixed with 4% paraformaldehyde for 10 min and permeabilized with 0.3% Triton X-100 for 5 min. After washing with PBS for three times, cardiomyocytes on glass coverslips were incubated with TUNEL reaction mixture (Cat. No. 12156792910, In Situ Cell Death Detection Kit, TMR Red, Roche, Indianapolis, IN) for 1 h at 37°C, in accordance with the manufacturer's instructions [46]. The number of TUNEL positive cells was counted in 4 random high-power fields per section.

2.10. ATP measurements and mitochondrial membrane potential observation

The ATP content in heart tissues was measured with an ATP Bioluminescent Assay Kit (Beyotime Biotechnology) in accordance with the manufacturer's instructions [47]. Cardiomyocytes seeded in 6-well plates were incubated with JC-1 probe (5 ng/ml, Beyotime Biotechnology) for 30 min at 37 °C in the dark, based on the manufacturer's instructions [48]. The mitochondrial membrane potential was visualized under the Zeiss LSM 700 confocal laser scanning microscope (Carl Zeiss, Germany). Images were captured using ZEN software (Carl Zeiss, Germany).

2.11. Statistical analysis

Data were analyzed using SPSS (Statistical Package for the Social Sciences) 16.0 (SPSS, Inc.). Differences between groups were analyzed using one-way analysis of variance (ANOVA) followed by Dunnett T3 post hoc when more than two groups were compared. A value of P < 0.05 was considered significant.

3. Results

3.1. Melatonin attenuates myocardial damage after renal ischemia-reperfusion injury (IRI)

First, we evaluated mouse renal IRI by analyzing blood levels of urea nitrogen (BUN) and creatinine (Cr). In comparison with the control sham group, mice with IRI showed a remarkable increase in BUN and Cr levels (Fig. 1A–B). Subsequently, we evaluated myocardial function 24 h after the renal surgery using echocardiography. As shown in Table 1, renal IRI had no influence on the parameters related to ventricular volume load, such as interventricular septum depth at end diastole (IVSD), interventricular septum depth at end systole (IVSs), left ventricular internal diameter at end diastole (LVIDd), left ventricular internal dimension at end systole (LVIDs), left ventricular posterior wall depth at end diastole (LVPWd), left ventricular posterior wall depth at end systole (LVPWs), left ventricular end diastolic volume (LVEDV), and left ventricular end systolic volume (LVESV). In addition, cardiac systolic indexes, such as left ventricular ejection fraction (LVEF) and left ventricular fractional shortening (LVFS) were not affected by the renal IRI. However, cardiac diastolic function, as assessed by using left ventricular mass (LVM) and E/A value, was reduced in mice after renal IRI surgery (Table 1). To determine the effect of melatonin on myocardial protection after renal damage, melatonin was injected into mice 30 min after renal IRI to exclude its possible influence on the extent of acute kidney injury. In comparison with the renal IRI group, melatonin improved the E/A value, and reduced LVM. These results indicate that cardiac diastolic function, rather than systolic property, is compromised after renal IRI, and that melatonin protects the cardiac diastolic function during CRS-3. To visualize the changes in myocardial tissues after renal IRI, we used HE staining and electron microscopy. As shown in Fig. 1C, myocardial swelling was evident in mice subjected to renal IRI. In addition, pathological injuries in mitochondria, such as mitochondrial swelling and cristae deformation (Fig. 1D), were also prominent in the renal IRI group. Importantly, melatonin attenuated the myocardial swelling and sustained the mitochondrial structure after IRI

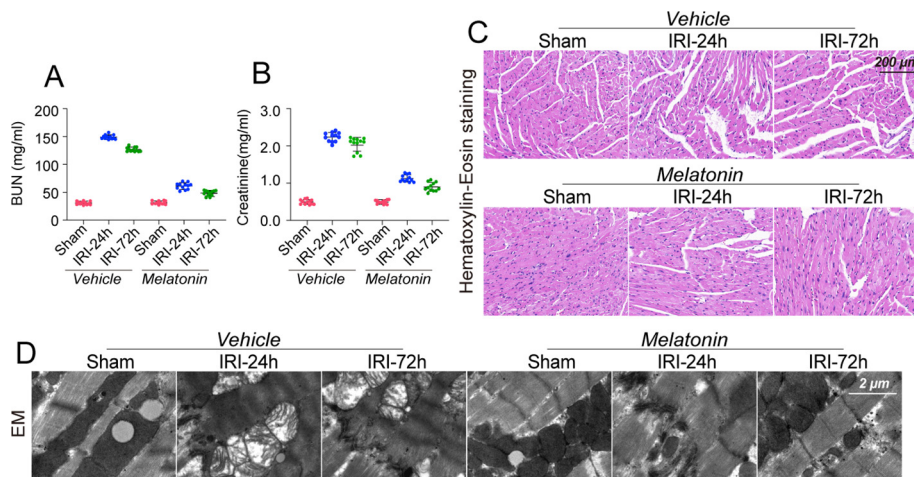


Fig. 1. Melatonin improves cardiac function in CRS-3. A–B. ELISA of BUN and Cr levels in blood after renal IRI. C. HE staining of myocardial structure. D. EM of myocardial ultra-structure. N = 6 mice per group; experiments were repeated three times. The data represent the mean ± SEM. *p < 0.05 vs. sham group.

(Fig. 1C–D). These results indicate that the cardiac diastolic function is depressed during CRS-3 in response to acute kidney injury, and that melatonin protects the heart function during CRS-3.

3.2. Melatonin improves mechanical parameters of cardiomyocytes in CRS-3

Next, signal ventricular cardiomyocytes were isolated from mice with IRI, and the beating frequencies and mechanical characteristics were analyzed *in vitro*. Neither IRI nor melatonin affected the average longitudinal length of cardiomyocytes (Fig. 2A). Although renal IRI caused a decrease in peaking shortening, maximal velocity of shortening (+dL/dt), and time-to-peak shortening (TPS) (Fig. 2B–F), the differences were not statistically significant. Interestingly, the maximal velocity of relengthening (–dL/dt) and the time-to-90% relengthening (TR90) were reduced by renal IRI surgery and returned to normal levels after melatonin treatment (Fig. 2B–F). These data indicate that cardiomyocyte relaxation index, rather than contraction, is regulated by melatonin during CRS-3.

3.3. Melatonin reduces myocardial inflammation and sustains cardiomyocyte viability in CRS-3

Since myocardial inflammation has been associated with myocardial edema [49], we analyzed expression of pro-inflammatory genes in mice after renal IRI. RNA analysis showed that the expression of pro-inflammatory genes was enhanced 24 h after renal IRI, and significantly augmented 72 h after renal IRI (Fig. 3A–C), coinciding with a late increase in the weight of the left ventricle. The protein levels of TNFα, IL-6, and TGFβ were also elevated in myocardium isolated from the renal IRI group (Fig. 3D–G). Melatonin decreased the pro-inflammatory proteins levels (Fig. 3D–G). Of note, these changes in myocardial inflammation were inversely correlated with cardiomyocyte viability, as evaluated via PI staining *in vivo*, and MTT assay *in vitro*. In the renal IRI-treated mice, the number of PI⁺ cardiomyocytes was higher than in the sham group (Fig. 3H–I), indicating the occurrence of cardiomyocyte death during CRS-3. Similarly, MTT assay-estimated cardiomyocyte viability was also reduced after acute kidney damage *in vitro* (Fig. 3J). Melatonin treatment favored cardiomyocyte survival, and increased cardiomyocyte viability *in vivo* and *in vitro* during CRS-3 (Fig. 3H–J). In addition, the expression of anti-oxidative genes nuclear factor erythroid 2-related factor 2 (Nrf2) and heme oxygenase-1 (HO-1) decreased after CRS-3, and increased to near-normal levels with melatonin treatment

Table 1
Cardiac function assessment through echocardiography after renal IR injury.

	Vehicle			Melatonin		
	Sham	IRI-24 h	IRI-72 h	Sham	IRI-24 h	IRI-72 h
IVSd (mm)	1.07 ± 0.04	0.99 ± 0.07	1.10 ± 0.06	1.03 ± 0.04	1.09 ± 0.06	1.06 ± 0.05
IVSs (mm)	1.29 ± 0.09	1.32 ± 1.01	1.31 ± 0.05	1.33 ± 0.08	1.29 ± 0.06	1.31 ± 0.09
IVIDd (mm)	3.34 ± 0.17	3.19 ± 0.19	3.29 ± 0.15	3.22 ± 0.17	3.31 ± 0.20	3.27 ± 0.14
IVIDs (mm)	2.48 ± 0.14	2.33 ± 0.17	2.49 ± 0.18	2.35 ± 0.12	2.44 ± 0.18	2.40 ± 0.16
IVPWd (mm)	0.84 ± 0.05	0.87 ± 0.07	0.85 ± 0.07	0.82 ± 0.06	0.86 ± 0.04	0.80 ± 0.05
IVPWS (mm)	1.22 ± 0.08	1.29 ± 0.14	1.19 ± 0.16	1.24 ± 0.10	1.16 ± 0.12	1.27 ± 0.15
LVESV (ul)	21.99 ± 3.16	21.07 ± 2.88	22.87 ± 3.56	21.89 ± 2.37	22.38 ± 3.01	20.97 ± 2.56
LVEDV (ul)	45.46 ± 5.31	52.30 ± 5.98	52.44 ± 6.22	47.98 ± 3.11	50.56 ± 4.38	51.73 ± 4.27
LVEF (%)	60 ± 2	55 ± 4	57 ± 3	57 ± 4	55 ± 5	59 ± 4
LVFS (%)	31 ± 3	29 ± 2	27 ± 4	30 ± 3	31 ± 2	19 ± 3
LVM (mg)	115.38 ± 8.83	120.83 ± 10.07	162.66 ± 15.74*	117.98 ± 9.34	116.33 ± 11.06	123.74 ± 10.83
E/A value	1.32 ± 0.21	1.29 ± 0.13	0.91 ± 0.11*	1.22 ± 0.12	1.28 ± 0.14	1.19 ± 0.11

*p < 0.05 vs. sham group.

IVSd: Interventricular septum depth at end diastole, IVSs: interventricular septum depth at end systole, LVIDd: left ventricular internal diameter at end diastole, LVIDs: left ventricular internal dimension at end systole, LVPWd: left ventricular posterior wall depth at end diastole, LVPWs: left ventricular posterior wall depth at end systole, LVEF: left ventricular ejection fraction, LVFS: left ventricular fractional shortening, LVM: left ventricular mass, LVEDV: left ventricular end diastolic volume, LVESV: left ventricular end systolic volume.

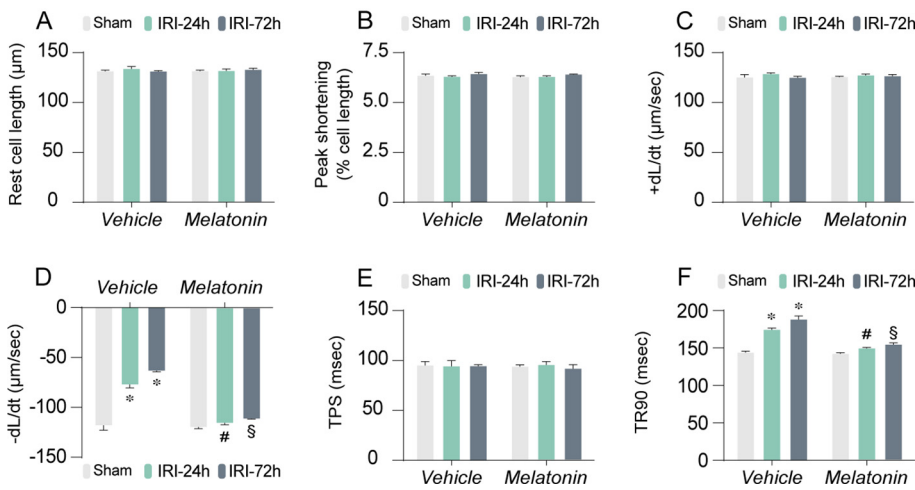


Fig. 2. Melatonin sustains cardiomyocyte mechanical parameters after renal IRI. A–F. The cardiomyocytes contractile properties in mice in the context of renal IRI. N = 70–80 cells from 2 mice per group and experiments were repeated three times. The data represent the mean ± SEM. *p < 0.05 vs. sham group, #p < 0.05 vs. IRI-24 h group; \$p < 0.05 vs. IRI-72 h group. + dL/dt is the maximal velocity of shortening, -dL/dt maximal velocity of re-lengthening, TPS time-to-peak shortening, TR90 time- to-90% relengthening.

(Fig. 3K–L). Thus, our results indicate that melatonin has anti-inflammatory and pro-survival effects that might explain its cardioprotective action in CRS-3-induced cardiac diastolic dysfunction and left ventricular edema.

3.4. Melatonin protects cardiomyocyte mitochondrial metabolism during CRS-3

The myocardial relaxation index is determined by mitochondria, which serve as a center for ATP generation by oxidative phosphorylation with the help of moderate $[Ca^{2+}]_m$ input. Oxidative stress induced by mitochondrial damage is also regarded as an initial signal for

myocardial inflammation [50]. In cardiomyocytes isolated from renal IRI-treated mice, the mitochondrial membrane potential (as evaluated via JC-1 assay) (Fig. 4A–B) and electron respiratory complex (ETC) activity (Fig. 4C–E) were reduced, but the reduction was reversed in cardiomyocytes isolated from melatonin-treated mice. The mitochondrial membrane potential reduction correlated with a drop in the total ATP content in cardiomyocytes in vitro (Fig. 4F). However, in the melatonin-treated cardiomyocytes, the ATP levels were sustained in vitro.

Recent studies have reported that mitochondrial fragmentation in cardiomyocytes, induced by renal IRI, damages cellular physiology through the production of reactive oxygen species and the promotion of

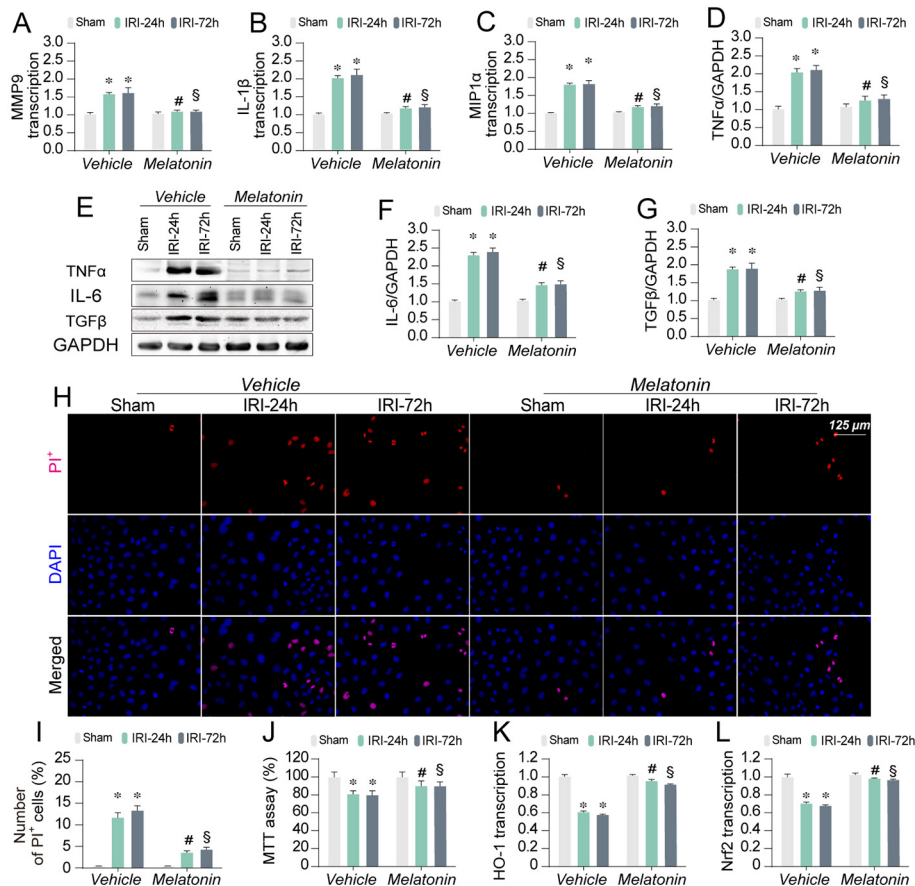


Fig. 3. Melatonin reduces myocardial inflammation after renal IRI. A–C. qRT-PCR of inflammatory genes analyzed in heart tissues after IRI. D–G. Western analysis of inflammatory proteins isolated from heart tissues after renal IRI. H–I. PI staining for cardiomyocyte death after renal IRI. The number of apoptotic cells was measured to determine the levels of cardiomyocyte death. J. MTT assay of cell viability in vitro after renal IRI. K–L. qRT-PCR of Nrf2 and HO-1 in cardiomyocytes. The data represent three independent experiments, and are expressed as the mean ± SEM. *p < 0.05 vs. sham group, #p < 0.05 vs. IRI-24 h group; \$p < 0.05 vs. IRI-72 h group.

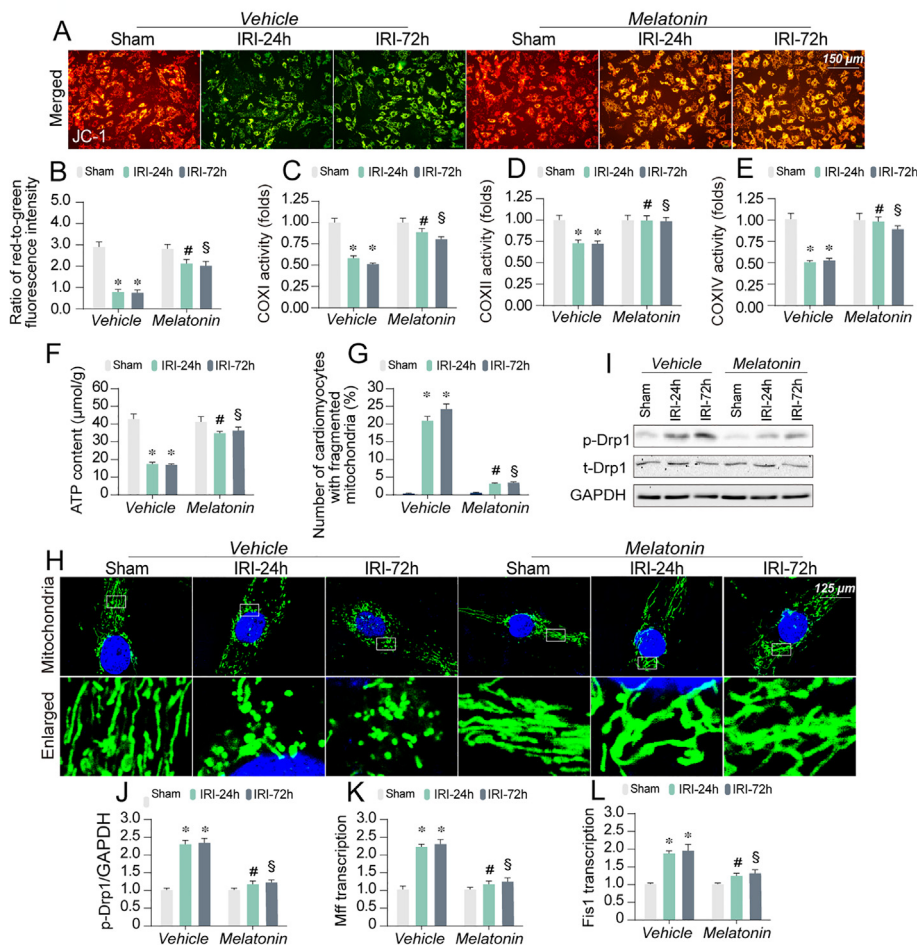


Fig. 4. Mitochondrial function is maintained by melatonin in CRS-3. A–B. Mitochondrial membrane potential was evaluated via JC-1 probe. The red-to-green fluorescence intensity was used to record the mitochondrial potential. C–E. ELISA of mitochondrial respiratory complex activity. Cardiomyocytes were isolated from mice after treatment with renal IRI. F–G. Immunofluorescence of mitochondrial fission. The number of cardiomyocytes with fragmented mitochondria was recorded. H. ATP production in cardiomyocytes isolated from mice treated with renal IRI. I–J. Western analysis of mitochondrial fission proteins isolated from heart tissues after renal IRI. K–L. qRT-PCR of mitochondrial fission-related genes in heart tissues after IRI. The data represent three independent experiments, and are expressed as the mean \pm SEM. * $p < 0.05$ vs. sham group, # $p < 0.05$ vs. IRI-24 h group; \$ $p < 0.05$ vs. IRI-72 h group. (For interpretation of the references to colour in this figure legend, the reader is referred to the web version of this article.)

mitochondria-dependent programmed cell death. In this study, the immunofluorescence of mitochondria demonstrated that renal IRI induced the cleavage of mitochondria from an elongated network into small spheres or rods (Fig. 4G–H). Moreover, the ratio of cardiomyocytes with fragmented mitochondria was elevated in response to the renal IRI (Fig. 4G–H). Melatonin treatment prevented the mitochondrial cleavage, and thus reduced the percentage of cardiomyocytes with fragmented mitochondria (Fig. 4G–H). In previous studies, we have investigated the molecular mechanisms governing mitochondrial fission of cardiomyocytes [33,46,48,51]. Here we show that renal IRI induces Drp1 phosphorylation (Fig. 4I–J), and increases expression of its receptors Mff and Fis1 (Fig. 4K–L) *in vivo*. Melatonin suppresses Drp1 phosphorylation and reduces Mff/Fis1 expression to near-normal levels (Fig. 4I–L). These results indicate that CRS-3 targets both mitochondrial function and cardiomyocyte structure, and that melatonin protects the mitochondrial cardiomyocyte homeostasis after acute renal IRI.

3.5. Melatonin reduces CRS-3-mediated cytoplasmic and mitochondrial calcium overload

Myocardial relaxation is a process in which the ER actively reabsorbs $[Ca^{2+}]_i$ to interrupt calcium-mediated cardiomyocyte contraction through consuming mitochondria-supplied ATP. Errors in this process can result in $[Ca^{2+}]_i$ overload, leading to cardiac diastolic dysfunction. Mitochondria are also involved in the maintenance of $[Ca^{2+}]_i$ homeostasis by buffering cytosolic Ca^{2+} when it rises to high levels [23,24]. Unfortunately, $[Ca^{2+}]_i$ overload is closely associated with $[Ca^{2+}]_m$ upregulation [52], which is followed by impaired TCA cycle and reduced ATP production. Reduction in ATP levels blunts ER-

mediated calcium recycling, an ATP-dependent calcium reflux against a concentration gradient. These two events, $[Ca^{2+}]_i$ overload and $[Ca^{2+}]_m$ upregulation, may exacerbate each other in a vicious cycle leading to cardiomyocyte dysfunction or death. In the present study, double-staining of $[Ca^{2+}]_i/[Ca^{2+}]_m$ demonstrated that renal IRI caused a significant rise in $[Ca^{2+}]_i/[Ca^{2+}]_m$ (Fig. 5A–C). However, the $[Ca^{2+}]_i$ overload was attenuated by BAPTA, a cell-permeable intracellular calcium chelator (Fig. 5A–C). Interestingly, BAPTA also reduced the $[Ca^{2+}]_m$ levels, indicating that $[Ca^{2+}]_i$ overload induces $[Ca^{2+}]_m$ upregulation (Fig. 5A–C). Notably, melatonin had a similar effect to ameliorate the $[Ca^{2+}]_i/[Ca^{2+}]_m$ imbalance.

At the molecular level, $[Ca^{2+}]_i$ is controlled by ER-expressed calcium channels, including RyR, IP3R, and SERCA. In our previous studies we found that IP3R is required for cardiomyocyte $[Ca^{2+}]_i$ in a model of myocardial IRI [23,24]. In the present study, we have further explored the IP3R function in CRS-3. Interestingly, renal IRI had no influence on IP3R gene expression (Fig. 5D), suggesting a possible post-transcriptional modification of IP3R in cardiomyocytes during CRS-3. Recent studies have shown that IP3R phosphorylation at Ser1756 enhances its ability to release calcium into cytoplasm [53,54]. Our results show that renal IRI increases the p-IP3R^{Ser1756} levels in cardiomyocytes, while melatonin suppresses the p-IP3R^{Ser1756} levels (Fig. 5E–F).

The concentration of $[Ca^{2+}]_m$ is determined by MCU and NCX; the former is a $[Ca^{2+}]_m$ input channel, and the latter is a $[Ca^{2+}]_m$ liberation protein [55]. Our results show that the MCU gene expression was upregulated, while the NCX expression remained the same in cardiomyocytes after renal IRI (Fig. 5G–H). Melatonin decreased the MCU mRNA levels (Fig. 5G–H). Together, these data demonstrate that renal IRI induces cardiomyocyte $[Ca^{2+}]_i/[Ca^{2+}]_m$ overload, and indicate

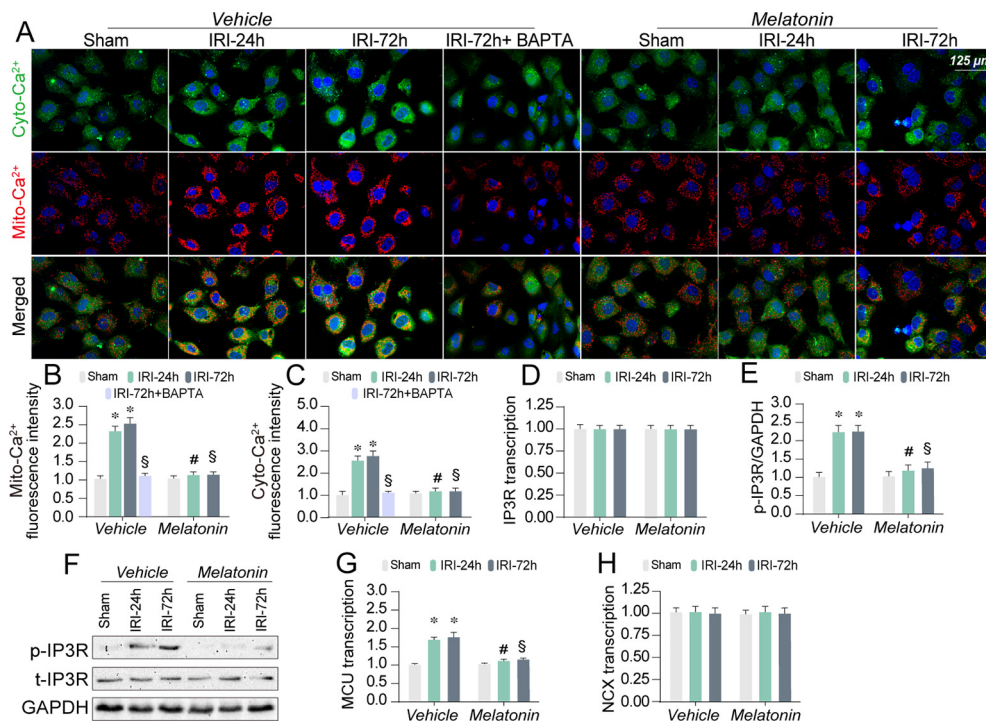


Fig. 5. Melatonin regulates mitochondrial and cytoplasmic calcium balance in CRS-3. A–C. Immunofluorescence of mitochondrial and cytoplasmic calcium overload in cardiomyocytes treated with and without melatonin. D. qRT-PCR of IP3R expression. E–F. Western blotting of IP3R phosphorylation at Ser1756. G–H. qRT-PCR of MUC and NCX expression. The data represent three independent experiments, and are expressed as the mean ± SEM. *p < 0.05 vs. sham group, #p < 0.05 vs. IRI-24 h group; \$p < 0.05 vs. IRI-72 h group.

that melatonin maintains $[Ca^{2+}]_i/[Ca^{2+}]_m$ transport by inhibiting IP3R phosphorylation and MCU transcription.

3.6. IP3R-MCU activation abolishes melatonin-mediated cardioprotection in vivo and in vitro

To verify that melatonin sustains cardiomyocytes' function through the IP3R-MCU axis, mice after renal IRI were injected with spermine, an agonist of MCU, or Xestospongin C, a selective inhibitor of IP3R. As shown in Table 2, although melatonin sustained the cardiac diastolic function after renal IRI, its cardioprotective effect was abrogated by spermine. Notably, Xestospongin C also protected the heart function after renal IRI. In cardiomyocytes isolated from mice after renal IRI, the cardiomyocyte relaxation index ($-dL/dt$ and TR90) was maintained by melatonin or Xestospongin C, but was aggravated after injection with spermine in the setting of CRS-3 (Fig. 6A–B). In addition to functional alterations, the cardiomyocyte viability was normalized by melatonin or Xestospongin C during CRS-3; however, this pro-survival action was absent following injection with spermine (Fig. 6C).

At the sub-cellular level, inhibition of IP3R maintained the mitochondrial performance (Fig. 6D–F), similarly to the protective effect of melatonin. However, activation of MCU attenuated the protective effects of melatonin on mitochondrial function, as evidenced by lower mitochondrial membrane potential (Fig. 6D–E) and reduced cellular ATP production (Fig. 6F) in spermine-treated cardiomyocytes in the presence of melatonin. Furthermore, mitochondrial fission recurred in cardiomyocytes after activation of the IP3R-MCU axis (Fig. 6G–H).

Table 2
Cardiac function assessment through echocardiography.

	Vehicle			Melatonin		
	Sham	IRI-72 h	IRI-72H + XC	Sham	IRI-72 h	IRI-72 h + Spe
LVM (mg)	116.75 ± 7.94	164.31 ± 14.97*	119.02 ± 8.14#	115.64 ± 7.02	117.24 ± 6.81	160.74 ± 10.24#
E/A value	1.29 ± 0.17	0.91 ± 0.10*	1.27 ± 0.18#	1.31 ± 0.17	1.28 ± 0.18	0.94 ± 0.09#

*p < 0.05 vs. sham group; #p < 0.05 vs. IRI-72 h group.
LVM: left ventricular mass.

Together, these results indicate that melatonin protects the cardiac function by repressing the IP3R-MCU signaling pathway.

4. Discussion

Our study shows that acute kidney injury primarily induces the cardiac diastolic dysfunction. Importantly, our data demonstrate, for the first time, the cardioprotective effect of melatonin in CRS-3. Two mechanisms might contribute to the cardiac damage during CRS-3: myocardial inflammation and cardiomyocyte viability reduction. In addition, mitochondrial energy metabolism and intracellular calcium dysregulation might contribute to the compromised cardiomyocyte relaxation. Our results show that renal IRI activates the IP3R-MCU pathway, resulting in $[Ca^{2+}]_i/[Ca^{2+}]_m$ overload. Importantly, melatonin decreases IP3R phosphorylation and MCU expression, thus reversing the intracellular calcium homeostasis, and sustaining the cardiomyocyte function. These novel data indicate that melatonin attenuates the mitochondrial damage and the relaxation dysfunction caused by calcium imbalance through the IP3R-MCU pathway, and thus plays an indispensable role in cardioprotection during CRS-3. Elucidation of the clinical benefits of melatonin in the prevention and treatment of CRS-3 may yield a more solid support for the use of melatonin in patients with coexisting cardiovascular and kidney disorders.

Although the concept of CRS has been clearly identified, our understanding of CRS-3 pathophysiology is limited. Oxidative stress, inflammation, metabolic alterations, and cardiomyocyte death have been proposed as possible mechanisms responsible for the cardiac damage

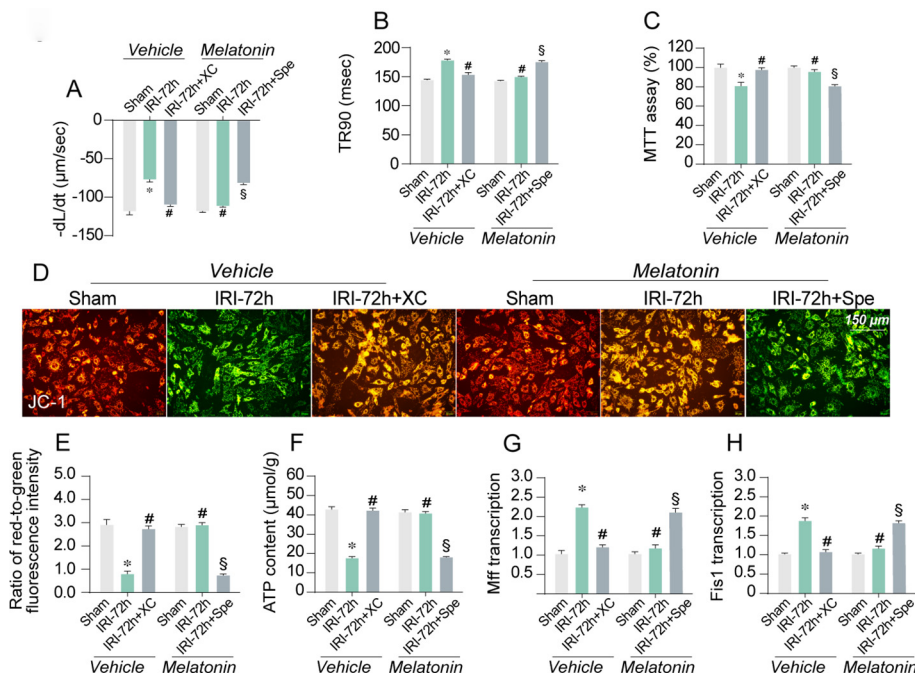


Fig. 6. Melatonin reduces myocardial damage via regulating IP3R-MCU pathway. A–B. Mice were treated with Xestospongin C (XC) or spermine (Spe) to block IP3R activation and MCU expression before melatonin treatment and renal IRI, respectively. C. Cell viability measured in cardiomyocytes isolated from mice treated with melatonin or after renal IRI. D–E. Mitochondrial membrane potential evaluated via JC-1 probe. The red-to-green fluorescence intensity was used to record the mitochondrial potential. F. ATP production determined in cardiomyocytes isolated from mice after renal IRI. G–H. qRT-PCR of mitochondrial fission-related genes measured in heart tissues after IRI. The data represent three independent experiments, and are expressed as the mean \pm SEM. * $p < 0.05$ vs. sham group, # $p < 0.05$ vs. IRI-272 h group; \$ $p < 0.05$ vs. melatonin + IRI-72 h group. (For interpretation of the references to colour in this figure legend, the reader is referred to the web version of this article.)

following acute kidney injury [7,66]. In line with previous studies, our results also indicate that inflammation, oxidative stress, and cardiomyocyte death are induced in the myocardium after renal IRI. Of note, since it is technically difficult to mimic CRS-3 in vitro, a fresh isolation of cardiomyocytes from renal IRI-treated mice is one of the methods to explore the mechanisms underlying cardiac damage. However, since cardiomyocyte isolation may affect its viability and trigger oxidative stress, these effects might underestimate the damage induced by renal IRI as well as the cardioprotection exerted by melatonin. Although the in vitro cardiomyocyte experiments were conducted 24 h after cardiomyocyte isolation, cell death was still obvious in cardiomyocytes isolated from renal IRI-treated mice, demonstrating that cardiomyocyte death is a critical downstream event in response to renal IRI. In addition, our results demonstrate that cardiac diastolic function rather than myocardial contraction is affected in mice receiving renal IRI; this phenotypic alteration may be secondary to acute kidney injury-mediated inflammation responses or hemodynamic changes because kidney dysfunction cannot directly trigger cardiomyocyte damage.

The mechanisms underlying the acute kidney injury-mediated cardiac diastolic dysfunction include inflammation-induced myocardial edema, mitochondrial bioenergetics depression, and intracellular calcium overload. Cardiomyocyte viability reduction and myocyte death may also contribute to diastolic dysfunction, although the cardiomyocyte death index is relatively low. In our study, there was a synchronous change between inflammation response (myocardial edema as assessed via EM) and left-ventricular weight increase. The ventricular wall stiffness induced by inflammation and edema may have limited cardiac relaxation. After supplementation with melatonin, myocardial inflammation was reduced, contributing to a reduction in left ventricular weight. Melatonin also improved mitochondrial metabolism and calcium homeostasis, actions that have been carefully explored in several previous studies [67,68].

Our results identify a novel signaling pathway regulated by melatonin in the setting of CRS-3. The IP3R-MCU axis is connected with the balance of $[Ca^{2+}]_i/[Ca^{2+}]_m$. Our data show that renal IRI does not affect IP3R transcription, but induces IP3R phosphorylation at Ser1756, and that this phosphorylation is inhibited by melatonin. Phosphorylation of IP3R at Ser1756 increases its ability to liberate calcium into cytoplasm [53,54], and this may explain the baseline

$[Ca^{2+}]_i$ overload. Notably, $[Ca^{2+}]_i$ overload may also result from SERCA inactivity because SERCA is an ATPase whose activity depends on the ATP content [69]. After exposure to renal IRI, mitochondrial metabolism and ATP production are impaired, and these effects may cause SERCA inactivation and then $[Ca^{2+}]_i$ overload. In fact, we discussed SERCA-induced $[Ca^{2+}]_i$ overload and melatonin-mediated SERCA reactivation in our previous studies of acute and chronic cardiovascular disorders [24,25,40]. In addition to IP3R phosphorylation, our data show that renal IRI increases MCU gene expression and that melatonin drastically represses the MCU expression through an undefined mechanism. MCU controls the input of $[Ca^{2+}]_i$ into mitochondria, and increased MCU expression results in mitochondrial metabolic arrest and mitochondrial fission [70,71]. By downregulating IP3R and MCU, melatonin controls the intracellular calcium transport, and attenuates the cardiomyocyte damage caused by abnormal calcium signaling.

In summary, using a mouse model of CRS-3, we identified the IP3R-MCU pathway as a novel mechanism by which acute kidney injury induces cardiac diastolic dysfunction in response to $[Ca^{2+}]_i/[Ca^{2+}]_m$ dysregulation and mitochondrial damage. In addition, our results show that melatonin prevents the early loss of cardiac diastolic function by normalizing the IP3R-MCU- $[Ca^{2+}]_i/[Ca^{2+}]_m$ signaling pathway, and indicate that it may serve as an attractive therapeutic drug for cardioprotection in CRS-3.

CRediT authorship contribution statement

Jin Wang: Visualization, Investigation, Data curation. **Sam Toan:** Writing - review & editing. **Ruibing Li:** Supervision, Data curation. **Hao Zhou:** Conceptualization, Methodology, Writing - original draft.

Acknowledgements

We thank Prof. Jun Ren in University of Wyoming and Prof. Yundai Chen in PLA General Hospital for their helpful discussions.

Funding source

This work was supported in part by China Postdoctoral Science Foundation (2019TQ0128) and the NSFC (81900252, 81770261,

81900254 and 91749128).

Contribution statement

HZ and JW involved in conception and design, performance of experiments, data analysis and interpretation, and manuscript preparation; RBL involved in the development of methodology, JW and RBL involved in the data acquisition, HZ involved in financial support, study supervision and final approval of manuscript.

References

- [1] S. Zununi Vahed, M. Ardalan, C. Ronco, Rein cardiaque: historical notes on cardiorenal syndrome, *Cardiorenal Med.* (2019) 1–4.
- [2] K.S. Shah, J.C. Fang, Is heart failure with preserved ejection fraction a kidney disorder? *Curr. Hypertens. Rep.* 21 (11) (2019) 86.
- [3] E.N. Ter Horst, P.A.J. Krijnen, N. Hakimzadeh, L. Robbers, A. Hirsch, R. Nijveldt, I. Lommerse, R.D. Fontijn, E. Meinster, R. Delewi, N. van Royen, F. Zijlstra, A.C. van Rossum, C.E. van der Schoot, Kraan T van der Pouw, A.J. Horrevoets, A.M. van der Laan, H.W.M. Niessen, J.J. Piek, Elevated monocyte-specific type I interferon signalling correlates positively with cardiac healing in myocardial infarct patients but interferon alpha application deteriorates myocardial healing in rats, *Basic Res. Cardiol.* 114 (1) (2018) 1.
- [4] J.W. Wang, Y. Ren, Z.G. Lu, J. Gao, C.C. Zhao, L.X. Li, M. Wei, The combination of nonthyroidal illness syndrome and renal dysfunction further increases mortality risk in patients with acute myocardial infarction: a prospective cohort study, *BMC Cardiovasc. Disord.* 19 (1) (2019) 50.
- [5] T. Honda, Q. He, F. Wang, A.N. Redington, Acute and chronic remote ischemic conditioning attenuate septic cardiomyopathy, improve cardiac output, protect systemic organs, and improve mortality in a lipopolysaccharide-induced sepsis model, *Basic Res. Cardiol.* 114 (3) (2019) 15.
- [6] N. Ohashi, S. Isobe, S. Ishigaki, T. Aoki, T. Matsuyama, T. Sato, T. Fujikura, A. Kato, H. Yasuda, Increased heart rate is associated with intrarenal renin-angiotensin system activation in chronic kidney disease patients, *Clin. Exp. Nephrol.* 23 (9) (2019) 1109–1118.
- [7] M. Trentin-Sonoda, F.M. Fratoni, C.V. da Cruz Junho, W.C. Silva, K. Panico, M.S. Carneiro-Ramos, Caspase-1 as Molecular Key in Cardiac Remodeling during Cardiorenal Syndrome Type 3 in the Murine Model, *Curr. Mol. Med.* (2019).
- [8] H. Takahama, T. Nishikimi, S. Takashio, T. Hayashi, C. Nagai-Okatani, T. Asada, A. Fujiwara, Y. Nakagawa, M. Amano, Y. Hamatani, A. Okada, M. Amaki, T. Hasegawa, H. Kanzaki, K. Nishimura, S. Yasuda, K. Kangawa, T. Anzai, N. Minamino, C. Izumi, Change in the NT-proBNP/Mature BNP Molar ratio precedes worsening renal function in patients with acute heart failure: a novel predictor candidate for cardiorenal syndrome, *J. Am. Heart Assoc.* 8 (17) (2019) e011468.
- [9] R. Ramchandra, D.T. Xing, M. Matear, G. Lambert, A.M. Allen, C.N. May, Neurohumoral interactions contributing to renal vasoconstriction and decreased renal blood flow in heart failure, *Am. J. Physiol. Regul. Integr. Comp. Physiol.* 317 (3) (2019) R386–R396.
- [10] Y. Xue, B. Xu, C. Su, Q. Han, T. Wang, W. Tang, Cardiorenal syndrome in incident peritoneal dialysis patients: What is its effect on patients' outcomes? *PLoS One* 14 (6) (2019) e0218082.
- [11] O.C. Baltatu, S. Senar, L.A. Campos, J. Cipolla-Neto, Cardioprotective melatonin: translating from proof-of-concept studies to therapeutic use, *Int. J. Mol. Sci.* 20 (18) (2019).
- [12] F. Nduhirabandi, G.J. Maarman, Melatonin in heart failure: a promising therapeutic strategy? *Molecules* 23 (7) (2018).
- [13] J. Zhang, L. Wang, W. Xie, S. Hu, H. Zhou, P. Zhu, H. Zhu, Melatonin attenuates ER stress and mitochondrial damage in septic cardiomyopathy: A new mechanism involving BAP31 upregulation and MAPK-ERK pathway, *J. Cell. Physiol.* (2019).
- [14] H. Ouyang, J. Zhong, J. Lu, Y. Zhong, Y. Hu, Y. Tan, Inhibitory effect of melatonin on Mst1 ameliorates myocarditis through attenuating ER stress and mitochondrial dysfunction, *J. Mol. Histol.* 50 (5) (2019) 405–415.
- [15] A. Guven, O. Yavuz, M. Cam, F. Ercan, N. Bukan, C. Comunoglu, Melatonin protects against epirubicin-induced cardiotoxicity, *Acta Histochem.* 109 (1) (2007) 52–60.
- [16] T. Nishihara, E. Yamamoto, D. Sueti, K. Fujisue, H. Usuku, F. Oike, M. Takae, Y. Arima, S. Araki, S. Takashio, T. Nakamura, S. Suzuki, K. Sakamoto, H. Soejima, H. Kawano, K. Kaikita, K. Tsujita, Clinical significance of serum magnesium levels in patients with heart failure with preserved ejection fraction, *Medicine (Baltimore)*. 98 (38) (2019) e17069.
- [17] N. Sumneang, S. Kumfu, J. Khameekae, N. Siri-Angkul, S. Fucharoen, S.C. Chattapakorn, N. Chattapakorn, Combined iron chelator with N-acetylcysteine exerts the greatest effect on improving cardiac calcium homeostasis in iron-overloaded thalassemic mice, *Toxicology* 427 (2019) 152289.
- [18] S. Stoll, J. Xi, B. Ma, C. Leimena, E.J. Behringer, G. Qin, H. Qiu, The valosin-containing protein protects the heart against pathological Ca²⁺ overload by modulating Ca²⁺ uptake proteins, *Toxicol. Sci.* (2019).
- [19] W. Mughal, M. Martens, J. Field, D. Chapman, J. Huang, S. Rattan, Y. Hai, K.G. Cheung, S. Kereliuk, A.R. West, L.K. Cole, G.M. Hatch, W. Diehl-Jones, R. Keijzer, V.W. Dolinsky, I.M. Dixon, M.S. Parmacek, J.W. Gordon, Myocardium regulates mitochondrial calcium homeostasis and prevents permeability transition, *Cell Death Differ.* 25 (10) (2018) 1732–1748.
- [20] J.Q. Kwong, The mitochondrial calcium uniporter in the heart: energetics and beyond, *J. Physiol.* 595 (12) (2017) 3743–3751.
- [21] H.M. Viola, L.C. Hool, How does calcium regulate mitochondrial energetics in the heart? – New insights, *Heart Lung Circ.* 23 (7) (2014) 602–609.
- [22] H. Zhou, J. Wang, P. Zhu, S. Hu, J. Ren, Ripk3 regulates cardiac microvascular reperfusion injury: The role of IP3R-dependent calcium overload, XO-mediated oxidative stress and F-actin/filopodia-based cellular migration, *Cell. Signal.* 45 (2018) 12–22.
- [23] Y. Zhang, H. Zhou, W. Wu, C. Shi, S. Hu, T. Yin, Q. Ma, T. Han, Y. Zhang, F. Tian, Y. Chen, Liraglutide protects cardiac microvascular endothelial cells against hypoxia/reoxygenation injury through the suppression of the SR-Ca(2+)-XO-ROS axis via activation of the GLP-1R/PI3K/Akt/survivin pathways, *Free Radical Biol. Med.* 95 (2016) 278–292.
- [24] H. Zhu, Q. Jin, Y. Li, Q. Ma, J. Wang, D. Li, H. Zhou, Y. Chen, Melatonin protected cardiac microvascular endothelial cells against oxidative stress injury via suppression of IP3R-[Ca(2+)]_c/VDAC-[Ca(2+)]_m axis by activation of MAPK/ERK signaling pathway, *Cell Stress Chaperones.* 23 (1) (2018) 101–113.
- [25] S. Hu, P. Zhu, H. Zhou, Y. Zhang, Y. Chen, Melatonin-Induced Protective Effects on Cardiomyocytes Against Reperfusion Injury Partly Through Modulation of IP3R and SERCA2a Via Activation of ERK1, *Arq. Bras. Cardiol.* 110 (1) (2018) 44–51.
- [26] H.M. Yeung, M.W. Hung, M.L. Fung, Melatonin ameliorates calcium homeostasis in myocardial and ischemia-reperfusion injury in chronically hypoxic rats, *J. Pineal Res.* 45 (4) (2008) 373–382.
- [27] B. Chovancova, S. Hudecova, L. Lenceseva, P. Babula, I. Rezuchova, A. Penesova, M. Grman, R. Moravcik, M. Zeman, O. Krizanova, Melatonin-Induced Changes in Cytosolic Calcium Might be Responsible for Apoptosis Induction in Tumour Cells, *Cell. Physiol. Biochem.* 44 (2) (2017) 763–777.
- [28] M.F. Pecenin, L. Borges-Pereira, J. Levano-Garcia, A. Budu, E. Alves, K. Mikoshiba, A. Thomas, C.R.S. Garcia, Blocking IP3 signal transduction pathways inhibits melatonin-induced Ca(2+) signals and impairs P. falciparum development and proliferation in erythrocytes, *Cell Calcium* 72 (2018) 81–90.
- [29] T.C. Cardoso, T.E. Pompeu, C.L.M. Silva, The P2Y1 receptor-mediated leukocyte adhesion to endothelial cells is inhibited by melatonin, *Purinergic Signal.* 13 (3) (2017) 331–338.
- [30] S. Xu, H. Pi, L. Zhang, N. Zhang, Y. Li, H. Zhang, J. Tang, H. Li, M. Feng, P. Deng, P. Guo, L. Tian, J. Xie, M. He, Y. Lu, M. Zhong, Y. Zhang, W. Wang, R.J. Reiter, Z. Yu, Z. Zhou, Melatonin prevents abnormal mitochondrial dynamics resulting from the neurotoxicity of cadmium by blocking calcium-dependent translocation of Drp1 to the mitochondria, *J. Pineal Res.* 60 (3) (2016) 291–302.
- [31] A. Agil, E.K. Elmahallawy, J.M. Rodriguez-Ferrer, A. Adem, S.M. Bastaki, I. Al-Abbad, Y.A. Fino Solano, M. Navarro-Alarcón, Melatonin increases intracellular calcium in the liver, muscle, white adipose tissues and pancreas of diabetic obese rats, *Food Funct.* 6 (8) (2015) 2671–2678.
- [32] M. Morell, J.I. Burgos, L.A. Gonano, Petroff M. Vila, AMPK-dependent nitric oxide release provides contractile support during hyperosmotic stress, *Basic Res. Cardiol.* 113 (1) (2018) 7.
- [33] H. Zhou, P. Zhu, J. Wang, H. Zhu, J. Ren, Y. Chen, Pathogenesis of cardiac ischemia reperfusion injury is associated with CK2 α -disturbed mitochondrial homeostasis via suppression of FUNDC1-related mitophagy, *Cell Death Differ.* 25 (6) (2018) 1080–1093.
- [34] N.L. Syn, P.L. Lim, L.R. Kong, L. Wang, A.L. Wong, C.M. Lim, T.K.S. Loh, G. Siemeister, B.C. Goh, W.S. Hsieh, Pan-CDK inhibition augments cisplatin lethality in nasopharyngeal carcinoma cell lines and xenograft models, *Signal Trans. Targeted Ther.* 3 (2018) 9.
- [35] K. Kohlstedt, C. Trouvain, T. Fromel, T. Mutersbach, R. Henschler, I. Fleming, Role of the angiotensin-converting enzyme in the G-CSF-induced mobilization of progenitor cells, *Basic Res. Cardiol.* 113 (3) (2018) 18.
- [36] M.M. Cortese-Krott, E. Mergia, C.M. Kramer, W. Luckstadt, J. Yang, G. Wolff, C. Panknin, T. Bracht, B. Sitek, J. Pernow, J.P. Stasch, M. Feilisch, D. Koelsing, M. Kelm, Identification of a soluble guanylate cyclase in RBCs: preserved activity in patients with coronary artery disease, *Redox Biol.* 14 (2018) 328–337.
- [37] A. Gandarillas, R. Molinuevo, N. Sanz-Gomez, Mammalian endoreplication emerges to reveal a potential developmental timer, *Cell Death Differ.* 25 (3) (2018) 471–476.
- [38] J. Beckendorf, M.M.G. van den Hoogenhof, J. Backs, Physiological and unappreciated roles of CaMKII in the heart, *Basic Res. Cardiol.* 113 (4) (2018) 29.
- [39] Q. Jin, R. Li, N. Hu, T. Xin, P. Zhu, S. Hu, S. Ma, H. Zhu, J. Ren, H. Zhou, DUSP1 alleviates cardiac ischemia/reperfusion injury by suppressing the Mff-required mitochondrial fission and Bnip3-related mitophagy via the JNK pathways, *Redox Biol.* 14 (2018) 576–587.
- [40] H. Zhou, Y. Yue, J. Wang, Q. Ma, Y. Chen, Melatonin therapy for diabetic cardiomyopathy: A mechanism involving Syk-mitochondrial complex I-SERCA pathway, *Cell. Signal.* 47 (2018) 88–100.
- [41] R. Xu, M. Garcia-Barros, S. Wen, F. Li, C.L. Lin, Y.A. Hannun, L.M. Obeid, C. Mao, Tumor suppressor p53 links ceramide metabolism to DNA damage response through alkaline ceramidase 2, *Cell Death Differ.* 25 (5) (2018) 841–856.
- [42] I.A.A. Batista, L.A. Helguero, Biological processes and signal transduction pathways regulated by the protein methyltransferase SETD7 and their significance in cancer, *Signal Trans. Targeted Ther.* 3 (2018) 19.
- [43] Y. Abukar, R. Ramchandra, S.G. Hood, M.J. McKinley, L.C. Booth, S.T. Yao, C.N. May, Increased cardiac sympathetic nerve activity in ovine heart failure is reduced by lesion of the area postrema, but not lamina terminalis, *Basic Res. Cardiol.* 113 (5) (2018) 35.
- [44] M.B. Afonso, P.M. Rodrigues, A.L. Simao, M.M. Gaspar, T. Carvalho, P. Borralho, J.M. Banales, R.E. Castro, C.M.P. Rodrigues, miRNA-21 ablation protects against liver injury and necroptosis in cholestasis, *Cell Death Differ.* 25 (5) (2018) 857–872.
- [45] L. Zhou, H. Zhang, K.J.A. Davies, H.J. Forman, Aging-related decline in the

- induction of Nrf2-regulated antioxidant genes in human bronchial epithelial cells, *Redox Biol.* 14 (2018) 35–40.
- [46] H. Zhou, J. Wang, P. Zhu, H. Zhu, S. Toan, S. Hu, J. Ren, Y. Chen, NR4A1 aggravates the cardiac microvascular ischemia reperfusion injury through suppressing FUNDC1-mediated mitophagy and promoting Mff-required mitochondrial fission by CK2alpha, *Basic Res. Cardiol.* 113 (4) (2018) 23.
- [47] P.R. Angelova, M. Barilani, C. Lovejoy, M. Dossena, M. Vigano, A. Seresini, D. Piga, S. Gandhi, G. Pezzoli, A.Y. Abramov, L. Lazzari, Mitochondrial dysfunction in Parkinsonian mesenchymal stem cells impairs differentiation, *Redox Biol.* 14 (2018) 474–484.
- [48] H. Zhou, C. Shi, S. Hu, H. Zhu, J. Ren, Y. Chen, BI1 is associated with microvascular protection in cardiac ischemia reperfusion injury via repressing Syk-Nox2-Drp1-mitochondrial fission pathways, *Angiogenesis* 21 (3) (2018) 599–615.
- [49] V.M. Ferreira, J. Schulz-Menger, G. Holmvang, C.M. Kramer, I. Carbone, U. Sechtem, I. Kindermann, M. Gutberlet, L.T. Cooper, P. Liu, M.G. Friedrich, Cardiovascular magnetic resonance in nonischemic myocardial inflammation: expert recommendations, *J. Am. Coll. Cardiol.* 72 (24) (2018) 3158–3176.
- [50] J. Zhong, Y. Tan, J. Lu, J. Liu, X. Xiao, P. Zhu, S. Chen, S. Zheng, Y. Chen, Y. Hu, Z. Guo, Therapeutic contribution of melatonin to the treatment of septic cardiomyopathy: A novel mechanism linking Ripk3-modified mitochondrial performance and endoplasmic reticulum function, *Redox Biol.* 26 (2019) 101287.
- [51] H. Zhou, S. Wang, P. Zhu, S. Hu, Y. Chen, J. Ren, Empagliflozin rescues diabetic myocardial microvascular injury via AMPK-mediated inhibition of mitochondrial fission, *Redox Biol.* 15 (2018) 335–346.
- [52] B. Delprat, L. Crouzier, T.P. Su, T. Maurice, At the Crossing of ER Stress and MAMs: A Key Role of Sigma-1 Receptor? *Adv. Exp. Med. Biol.* 1131 (2020) 699–718.
- [53] L. Gomez, P.A. Thiebaut, M. Paillard, S. Ducreux, M. Abrial, C. Crola Da Silva, A. Durand, M.R. Alam, F. Van Coppenolle, S.S. Sheu, M. Ovize, The SR/ER-mitochondria calcium crosstalk is regulated by GSK3beta during reperfusion injury, *Cell Death Differ.* 22 (11) (2015) 1890.
- [54] L.S. Haug, V. Jensen, O. Hvalby, S.I. Walaas, A.C. Ostvold, Phosphorylation of the inositol 1,4,5-trisphosphate receptor by cyclic nucleotide-dependent kinases in vitro and in rat cerebellar slices in situ, *J. Biol. Chem.* 274 (11) (1999) 7467–7473.
- [55] C. Cui, R. Merritt, L. Fu, Z. Pan, Targeting calcium signaling in cancer therapy, *Acta Pharm. Sin. B* 7 (1) (2017) 3–17.
- [66] S.M. Bagshaw, E.A. Hoste, B. Braam, C. Briguori, J.A. Kellum, P.A. McCullough, C. Ronco, Cardiorenal syndrome type 3: pathophysiologic and epidemiologic considerations, *Contrib. Nephrol.* 182 (2013) 137–157.
- [67] S. Wang, W. Bian, J. Zhen, L. Zhao, W. Chen, Melatonin-Mediated Pak2 Activation Reduces Cardiomyocyte Death Through Suppressing Hypoxia Reoxygenation Injury-Induced Endoplasmic Reticulum Stress, *J. Cardiovasc. Pharmacol.* 74 (1) (2019) 20–29.
- [68] Z.S. Ataizi, K. Ertlav, M. Naziroglu, Mitochondrial oxidative stress-induced brain and hippocampus apoptosis decrease through modulation of caspase activity, Ca (2+) influx and inflammatory cytokine molecular pathways in the docetaxel-treated mice by melatonin and selenium treatments, *Metab. Brain Dis.* 34 (4) (2019) 1077–1089.
- [69] F. Tadini-Buoninsegni, S. Smeazzetto, R. Galdani, M.R. Moncelli, Drug Interactions With the Ca(2+)-ATPase From Sarco(Endo)Plasmic Reticulum (SERCA), *Front. Mol. Biosci.* 5 (2018) 36.
- [70] K.N. Belosludtsev, M.V. Dubinin, N.V. Belosludtseva, G.D. Mironova, Mitochondrial Ca2+ transport: mechanisms, molecular structures, and role in cells, *Biochemistry (Mosc.)* 84 (6) (2019) 593–607.
- [71] Giorgia Pallafacchina, Sofia Zanin, Rosario Rizzuto, Recent advances in the molecular mechanism of mitochondrial calcium uptake, *Fl000Res* 7 (2018) 1858.